Hydraulic-turbine start-up with " S-shaped " characteristic

Hugo Mesnage, Mazen Alamir, Nicolas Perrissin-Fabert, Quentin Alloin, Seddik Bacha

▶ **To cite this version:**

Hugo Mesnage, Mazen Alamir, Nicolas Perrissin-Fabert, Quentin Alloin, Seddik Bacha. Hydraulic-turbine start-up with " S-shaped " characteristic. ECC 2015 - 14th European Control Conference, Jul 2015, Linz, Austria. hal-01250201

HAL Id: hal-01250201
https://hal.science/hal-01250201

Submitted on 4 Jan 2016

HAL is a multi-disciplinary open access archive for the deposit and dissemination of scientific research documents, whether they are published or not. The documents may come from teaching and research institutions in France or abroad, or from public or private research centers.

L'archive ouverte pluridisciplinaire **HAL**, est destinée au dépôt et à la diffusion de documents scientifiques de niveau recherche, publiés ou non, émanant des établissements d'enseignement et de recherche français ou étrangers, des laboratoires publics ou privés.

Hydraulic-turbine start-up with "S-shaped" characteristic

Hugo Mesnage[1], Mazen Alamir[2], Nicolas Perrissin-Fabert[3], Quentin Alloin[3], Seddik Bacha[4]

***Abstract*— Fast response of hydraulic turbines is a key condition for the integration of renewable sources of energy. In this paper, a new start-up strategy is proposed for hydraulic turbines prone to "S" instability. This method is based on a complete nonlinear model of the turbine together with the upstream water pipe. More precisely, the control strategy is based on a gain scheduling approach that is computed using finite horizon predictive control. This yields a state feedback control law that tracks a time-optimal trajectory that is computed based on the nonlinear model of the system. Simulations are shown to assess the efficiency of the proposed law and its robustness to model discrepancies.**

Nomenclature

Symbol	Definition	Unit
H	net head/pressure at the bounds of the turbine	m
Q	flow in the turbine	m^3/s
Ω	rotational speed of the turbine	rd/s
γ	guide vanes' opening	$\%$
T	hydraulic torque on the runner	$N.m$
t_e	wave travel time in penstock	s
t_w	water starting time in penstock	s
ξ	state space vector for the penstock	
H_g	gross head of the plant (constant)	$> 100m$
x^d	desired steady state value of x	
D	diameter of the runner	m

I. INTRODUCTION

The need for energy storage to support intermittent renewable sources such as solar or wind is mandatory for their successful integration. If Diesel engine-based solutions [1] are excluded for straightforward environmental reasons, batteries and super-capacitor storage are generally viewed as power providers that are suitable for short and fast transients but which are not convenient when high amount of energy is needed. Hydro-electric conversion seems to be the unique clean way to compensate the intermittent nature of wind and solar energy. This is done by converting the potential energy of the upstream water in rotational kinetic energy in the turbine runner, and then converting it to electricity via a generator. When used as a pump, the same runner enables the storage of energy under its potential form, and can therefore support the integration of renewable sources.

Nevertheless, the use of hydraulic storage as a secondary source induces some new paradigms:

- The first concerns the start-up response time of the hydraulic turbine. This is the time necessary to drive the turbine from rest towards the connection-to-grid rotational speed. In our problem, the most spread, and studied, topology consists in a synchronous machine working at constant speed when linked to the grid. Thus, we need to achieve a stabilized 0.2% response over speed before connecting to grid [3]. Fast start-up operations that enable a rapid voltage recovery is more crucial than ever.

- Then comes the will of power plant operator to work in increasingly wide operation modes, namely the so-called "S" characteristics. The S-shaped characteristic of the turbine depends mainly on the hydraulic design of the runner. It involves power instability at the load-free rotational speed when the upstream pressure is in its lower range. This power instability leads to rotational speed instabilities before linking the machine to the grid and as we need a very tight stabilization of the speed ($\pm 0.2\%$), it can prevent the start-up of a plant. This phenomenon can be handled with the misalignment of guide vanes (MGV) that changes and stabilizes over speed the characteristic of the turbine [4]. The aim of this paper is to propose a control law that can work in the "S" without MGV that for operational reasons is not always easy to implement. This requires tighter control of the hydraulic system for every operating mode unlike in standard operational [5] conditions because of the inherent instability of the system in these areas.

- A third point would be the aim of Alstom to always provide better efficiency runners. Indeed, the sharper design of turbine-pump runners in its main operation modes can increase phenomenon such as the "S".

For all these reasons, a new control approach is needed which is the aim of the present paper which addresses the first above mentioned issue, namely, the design of minimum-time start-up control and proposes an answer to the stabilization in the "S". This methodology is based on the tracking of a stabilizing trajectory computed using a detailed nonlinear model of the plant.

The paper is organized as follow: First, the dynamic

[1]Hugo Mesnage is conducting his Phd's thesis research at Gipsa-lab with the support of Alstom Renewable Power Hydro and G2Elab in Grenoble hugo.mesnage@gipsa-lab.fr

[2]Mazen Alamir is Research director at Gipsa-Lab, Control Systems Department mazen.alamir@gipsa-lab.grenoble-inp.fr

[3] Nicolas Perrissin-Fabert and Quentin Alloin are research engineer at Alstom Renewable Power Hydro, R&D Process Control & Monitoring nicolas.perrissin-fabert@power.alstom.com quentin.alloin@power.alstom.com

[4]Seddik Bacha is Research director at G2Elab. Seddik.Bacha@g2elab.grenoble-inp.fr

model is given in section II. Section III clearly states the start-up control problem. Section IV analyses the system and proposes a trajectory that enables a full stabilization for coupling. Section V proposes a predictive control-based gain scheduling feedback and validates it through some simulation in the nominal case and in the presence of model discrepancy. Finally, section VI concludes the paper and gives hints for further investigations.

II. Modelisation

In this section, a detailed model of the plant is proposed by connecting together a model for the penstock and a model for the turbines. This is explained in the two following sections.

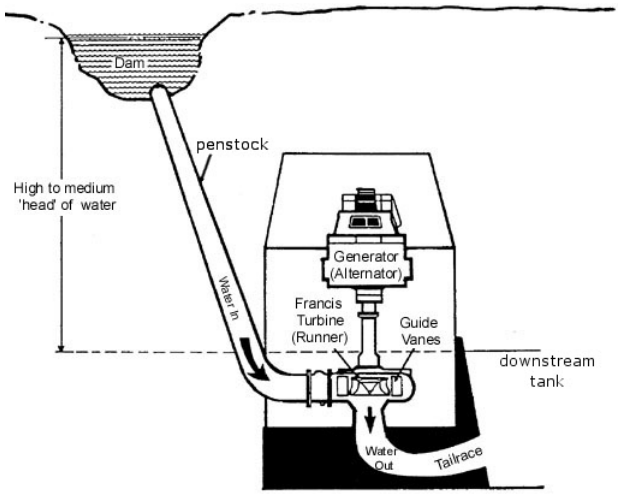

Fig. 1. The hydraulic plant

A. Penstock

It is considered here a medium to high-head plant as shown in figure 1. It has an upstream circuit made of one linear and constant section penstock. The penstock is defined by its water starting time t_w and its wave travel time t_e.

$$t_e = \frac{L}{a} \quad ; \quad t_w = \frac{L}{g \cdot A} \tag{1}$$

with,

A	section of the penstock
a	wave speed in the penstock
L	length of the pipe
g	acceleration of gravity

The following assumptions are used in the derivation of the penstock model: 1) the pipe is uniform and flow is one-dimensional; for quasi-incompressible fluids, the velocity and pressure distributions are uniform in each cross section of the conduit. 2) pipe deformations are proportional to the stresses (Hooke's law) and the liquid compressibility effects can be characterized by a constant bulk modulus. 3) no vaporization of the liquid occurs during the hydraulic transient. 4) the hydraulic friction losses are neglected. 5) no distributed lateral flows are considered.

It is then shown in [6] that the transfer function between the flow Q in the turbine and the head H at its boundaries can be given by the following expression in the Laplace domain:

$$\frac{\partial H}{\partial Q}(s) = -\frac{t_w}{t_e} \cdot tanh(s \cdot t_e) \tag{2}$$

Moreover, the transfer function giving the flow rate and water pressure of upstream inlet in terms of the downstream quantities is given by [6]:

$$\begin{pmatrix} h_U(s) \\ q_U(s) \end{pmatrix} = \begin{pmatrix} cosh(s \cdot t_e) & -\frac{t_w}{t_e} \cdot sinh(s \cdot t_e) \\ -\frac{t_e}{t_w} \cdot \sinh(s \cdot t_e) & cosh(s \cdot t_e) \end{pmatrix} \cdot \begin{pmatrix} h_D(s) \\ q_D(s) \end{pmatrix}$$

Therefore, it is possible to write the transfer function for a combination of linear and constant section penstocks in series. For the rest of the paper, a linear, fixed step, high order, representation of our penstock is considered that is computed according to the series expansion of (2):

$$\begin{array}{ll} \xi^+ & = A_\xi \cdot \xi + B_\xi \cdot Q \\ H & = C_\xi \cdot \xi + D_\xi \cdot Q + H_g \end{array} \tag{3}$$

where the pressure H between the bounds of the runner takes into account, a constant static gross head H_g relating to the heights of water in the upstream and downstream tank, and a dynamic evolution of pressure ($C_\xi \cdot \xi + D_\xi \cdot Q$) relating to the flow in the runner.

Figure 2 shows that the series expansion enables a good representation of the penstock in the low frequencies. The high frequencies would naturally not be excited by a limited bandwidth actuator. Moreover, the neglected hydraulic friction losses naturally attenuates those high frequencies. Note also that the first resonance peak is located at pulsation $(a\pi)/(2L)$ [a is the wave speed in the penstock, L is the length of the pipe]. Therefore, the longer the pipe is, the lower this first peak, and a higher truncation order of representation of the pipe is needed to cover up the bandwidth of the actuator.

B. Turbine

Unlike standard linear models of the hydro-turbine used when connected to the grid [7], we will pay a special attention to the dynamic of the turbine for start-up operations. This is necessary because we need a precise idea of the dynamic of this system on the whole range of operation in order to achieve a good control. The hydraulic-turbine dynamic is known through its hill-chart characteristic. This nonlinear characteristic (figure 3) relates the pressure H, the flow Q, the rotational speed Ω, the guide vanes opening γ and the torque T. The runner comes in consideration on two levels: on one hand it enables the computation of the torque T and on the other hand, it gives us access to the flow Q in the runner. The hill-charts characteristics of runner prone to "S" instabilities exhibit a possible undetermination: in the "S", for one rotational speed, guide vanes opening and pressure, there can be several associated flow rates. We choose thus a suterian representation [8] of the hill-chart to remove this

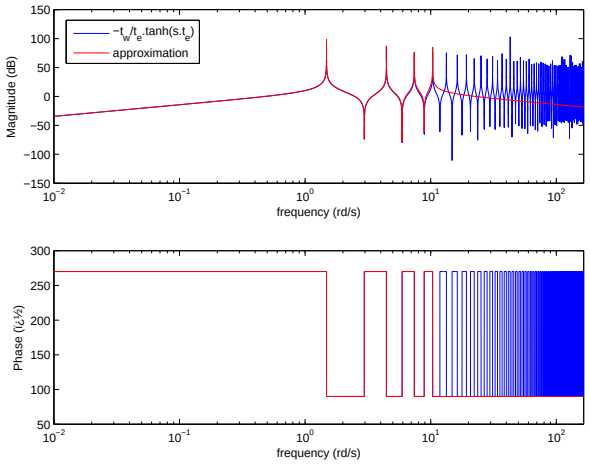

Fig. 2. Bode diagrams of the transfer function (2) and its approximation by a truncated series (3).

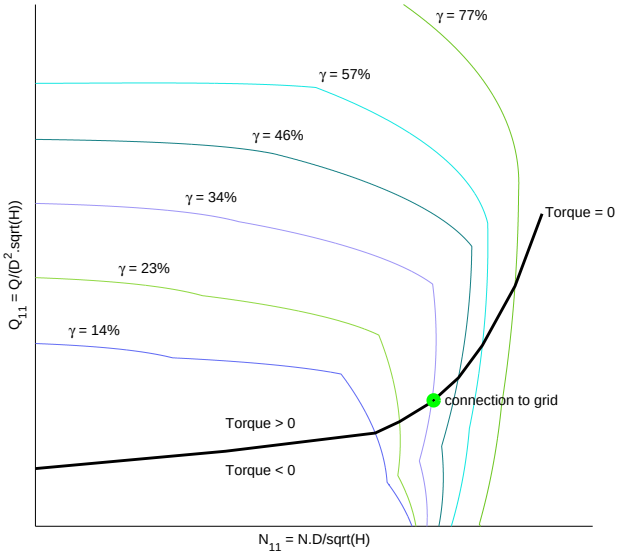

Fig. 3. example of a hill-chart- characteristic prone to "S" instability at connection-to-grid rotational speed

undetermination. These two relations can be shortly written as follows:

$$\begin{aligned} T &:= w_1(H,Q,\Omega,\gamma) \\ Q &:= w_2(H,Q,\Omega,\gamma) \end{aligned} \tag{4}$$

Note that Q is defined through nonlinear algebraic equation $Q := w_2(H,Q,\Omega,\gamma)$. In simulation, in order to avoid resolving this equation at every step, we associate to Q the following dynamic:

$$\dot{Q} = -\lambda_Q \cdot (Q - w_2(H,Q,\Omega,\gamma)) \tag{5}$$

with sufficiently high λ_Q. Finally, the dynamic of the rotational speed Ω is given by:

$$\dot{\Omega} = \frac{1}{J} \cdot (T - frott \cdot \Omega) \tag{6}$$

where J is the inertia of the runner while $frott$ is the friction coefficient.

III. The "S" start-up problem

This paper focuses on the start-up of turbines prone to "S" instability. This instability appears for low head, no-torque for the connection-to-grid rotational speed. As illustrated on the hill-chart shown in figure 3, this instability is characterized by the following inequality:

$$\left.\frac{\partial \dot{\Omega}}{\partial \Omega}\right|_{\gamma,Q,H} > 0 \tag{7}$$

The oscillations in the pipe naturally powers this instability and this instability powers the oscillations in the pipe in a way that makes difficult with a limited bandwidth actuator to recover a steady state in the "S" for some level of initial tracking error. The idea for resolving the start-up with the "S" unstability comes in two parts :

- find a "steering admissible trajectory" that brings the whole state of the system at time t_f to a suitable steady state for the pipe and the runner while meeting the actuator limitations.
- track the processed trajectory and stabilize the global system around steady state.

IV. Admissible trajectory for start-up in "S"

In this section, it is shown that the steering trajectory mentioned in the preceding section can be obtained through a polynomial parametrization of the trajectory of the head $H(\cdot)$ since all the other state variables can be induced from this trajectory as it is shown in the sequel. These steps are successfully described in the following sections.

A. Head trajectory $H(t)$

We are looking here for a trajectory that brings the initial pipe state $\xi(t_0)$ to the desired $\xi(t_f) = \xi^d \in \mathbb{R}^N$ in a finite time t_f, such that $\dot{\xi}^d = A_\xi \cdot \xi^d + B_\xi \cdot Q^d = 0$ [see (3)]. The trajectory $H(t)$ is then constrained at t_0 and at t_f together with its $N-1$-first derivatives. Note that beside these constraints that are intended to deliver a smooth trajectory that does not excite the unstable modes, this trajectory must be such that the resulting final speed and the resulting final flow rate are compatible with the unique open-loop unstable steady state (in the S) that is the reason why additional degrees of freedom must be added. This is done by defining a tuning vector at $t_C = \frac{t_0+t_f}{2}$ such that the r.h.s of the following equation can be used as tuning parameters to achieve these objectives:

$$\begin{pmatrix} H(t_C) \\ \dot{H}(t_C) \\ \vdots \\ H(t_C)^{(N_C-1)} \end{pmatrix} = \begin{pmatrix} c_0 \\ c_1 \\ \vdots \\ c_{N_C-1} \end{pmatrix} \tag{8}$$

where $H^{(i)}(t)$ the i^{th} derivative of H at time t.

$H(t)$ can then be parametrized by a polynomial of order $(2\cdot N+N_C)$. In what follows, the value $N_C=2$ is considered and the corresponding degrees of freedom c_0 and c_1 are used to enforce the final values of the flow Q^d and final value of the rotational speed Ω^d.
We note here that the $\circ^d$ variables are used to designate the targeted steady state participating in the balance-point of our system for start-up.

B. Flow rate trajectory $Q(t)$

Thanks to the linear equation (3) that links $H(t)$ and $Q(t)$, one can link the trajectories of these two variables through the equation

$$\begin{pmatrix} H_k \\ H_{k+1} \\ \vdots \\ H_{k+M-1} \end{pmatrix} = \Phi_M \cdot \xi_k + \Psi_M \cdot \begin{pmatrix} Q_k \\ Q_{k+1} \\ \vdots \\ Q_{k+M-1} \end{pmatrix}$$

where

$$\Phi_M = \begin{pmatrix} C_\xi \\ C_\xi A_\xi \\ \vdots \\ C_\xi A_\xi^{M-1} \end{pmatrix}$$

$$\Psi_M = \begin{pmatrix} D_\xi & 0 & \dots & 0 & 0 \\ C_\xi B_\xi & D_\xi & \dots & 0 & 0 \\ C_\xi A_\xi B_\xi & C_\xi B_\xi & \dots & 0 & 0 \\ \vdots & \vdots & \dots & D_\xi & 0 \\ C_\xi A_\xi^{M-2} B_\xi & C_\xi A_\xi^{M-3} B_\xi & \dots & C_\xi B_\xi & D_\xi \end{pmatrix}$$

therefore

$$\begin{pmatrix} Q_k \\ Q_{k+1} \\ \vdots \\ Q_{k+M-1} \end{pmatrix} = \Psi_M^{-1} \cdot \left(\begin{pmatrix} H_k \\ H_{k+1} \\ \vdots \\ H_{k+M-1} \end{pmatrix} - \Phi_M \cdot \xi_k \right) \quad (9)$$

This relation shows that for any given trajectory of H, the trajectory of Q can be computed. Using this, the final values of $Q(t_f)=Q^d$ can be enforced by appropriately choosing the coefficient c_0 involved in (8). By doing so, c_0 becomes dependent on the only remaining free parameter c_1.

C. Rotational speed trajectory $\Omega(t)$

Recall that Q is solution of the algebraic equation $Q = w_2(H,Q,\Omega,\gamma)$. This means that for any chosen candidate trajectory of $H(\cdot)$ [and hence of Q through (9)], the corresponding trajectory of the valve opening γ is only function of t and Ω, namely:

$$\gamma(\Omega,t) \leftarrow Solve[Q(t) - w_2(H(t),Q(t),\Omega,\gamma) = 0]$$

Injecting this in the dynamic equation of the speed (6) gives an autonomous equation in Ω [once $H(\cdot)$ is chosen]:

$$\dot{\Omega} = \frac{1}{J} \cdot [w_1(H(t),Q(t),\Omega,\gamma(\Omega,t)) - frott \cdot \Omega] \quad (10)$$

Integrating this equation gives the final value of the speed $\Omega(t_f)$ which depends on the only remaining parameter c_1 involved in (8). The latter can then be tuned in order to obtain the desired final speed $\Omega(t_f)=\Omega^d$.

The above process is completely defined for a given value of the final time t_f. The effectively selected trajectory is then obtained by dichotomy search over the final time t_f in order to respect the feasibility constraints. Indeed, by monitoring t_f, it is possible to slow down the dynamic or speed it up. Therefore it will be easy to define a trajectory that respects the predefined constraints of the system such as actuator dynamic, maximum values of pressure, maximum value for torque, etc. Moreover, the smoothness of such start-up ensures low mechanic stress on the runner which is an important requirement for the system life-time. Note that by computing the appropriate t_f, a sub-optimal solution is quickly derived for the problem of constrained minimum time path generation. The whole trajectory generation can be computed in under $1sec$ when well initialized.

D. The need for feedback

Although the trajectory computed in the preceding section is based on a nonlinear detailed model of the plant, the unstable character of the system prevents its use in open-loop even in start mode. In order to highlight this fact, open-lop simulations are shown in Figure 4 with small model discrepancies. More precisely, Figure 4 shows the desired trajectory from $t_0=0$ to $t_f=30$ sec and the open-loop trajectory obtained by simulating the system (with the computed $\gamma(\cdot)$) for the perturbed model given by:

$$\begin{pmatrix} \dot{\xi} \\ \dot{Q} \\ \dot{\Omega} \end{pmatrix} = \begin{pmatrix} A_\xi & 0 & 0 \\ 0 & -\lambda_Q & 0 \\ 0 & 0 & \frac{-frott}{J} \cdot \Omega \end{pmatrix} (\mathbb{I}+P) \cdot \begin{pmatrix} \xi \\ Q \\ \Omega \end{pmatrix} + \begin{pmatrix} 0 \\ p_1 \cdot \lambda_Q \cdot w_2(H,Q,\Omega,\gamma) \\ p_2 \cdot \frac{1}{J} \cdot w_1(H,Q,\Omega,\gamma) \end{pmatrix} \quad (11)$$

with, P, p_1 and p_2 coming from a normal distribution with mean 0 and standard deviation of 5%
Based on this observation, a feedback strategy is developed in the next section in order to guarantee a robust tracking of the pre-computed time optimal trajectory.

V. Gain scheduling

A. Computation of the gain

In this section the system is linearized along the precomputed trajectory and an appropriate time-dependent gain is computed using finite horizon model predictive control strategy. The gain is therefore to be applied to the tracking error on the state vector. Note that this implicitly assumes that the state vector is measurable. The construction of the dynamic observer is not analyzed here and will be investigated later on.

Let us adopt the following notation:

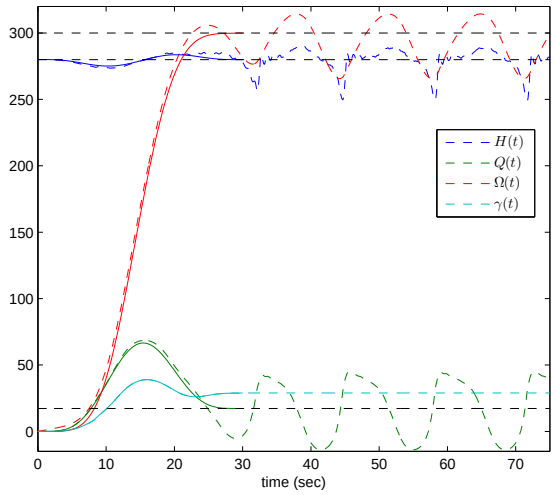

Fig. 4. The need for closed-loop start. Desired trajectory computed trough process described in IV (solid line) and open-loop simulated trajectory using the disturbed system (11) (dashed line)

- $X = \begin{pmatrix} \xi^T & Q & \Omega \end{pmatrix}^T \in \mathbb{R}^n$, it is the actual state of the system.
- $\tilde{X} = \begin{pmatrix} \tilde{\xi}^T & \tilde{Q} & \tilde{\Omega} \end{pmatrix}^T \in \mathbb{R}^n$, it is the desired state of the system computed thanks to the algorithm described in section IV.
- to simplify the notation, subscript k refers to the sampling instant.

The dynamic system together with the ideal one can be shortly given by:

$$\begin{array}{ll} X_{k+1} & = f(X_k, \gamma_k) \\ \tilde{X}_{k+1} & = f(\tilde{X}_k, \tilde{\gamma}_k) \end{array} \tag{12}$$

The error $e_k = \tilde{X}_k - X_k$ shows the following linearized dynamic:

$$\begin{array}{rcccc} e_{k+1} & = & \frac{\partial f}{\partial X}(\tilde{X}_k, \tilde{\gamma}_k) \cdot e_k & + & \frac{\partial f}{\partial \gamma}(\tilde{X}_k, \tilde{\gamma}_k) \cdot v_k \\ & = & A_k \cdot e_k & + & B_k \cdot v_k \end{array}$$

where $v_k = \tilde{\gamma}_k - \gamma_k$, v_k denotes the value of corrective feedback at instant k. In order to differentiate the weighting on the different components of e, we introduce a square weighting matrix W and define the regulated variable z by:

$$z_k = W \cdot e_k$$

This induces the following dynamic on the regulated variable z:

$$\begin{array}{rcccc} z_{k+1} & = & W \cdot A_k \cdot W^{-1} \cdot z_k & + & W \cdot B_k \cdot v_k \\ & = & \bar{A}_k \cdot z_k & + & \bar{B}_k \cdot v_k \end{array}$$

Moreover, if we choose prediction horizon $L \in \mathbb{N}$ then the evolution of z can be given in term of the initial value z_k and the set of future controls according to:

$$\begin{pmatrix} z_k \\ z_{k+1} \\ \vdots \\ z_{k+L-1} \end{pmatrix} = \Phi_k \cdot z_k + \Psi_k \cdot \begin{pmatrix} v_k \\ v_{k+1} \\ \vdots \\ v_{k+L-2} \end{pmatrix} \tag{13}$$

where Φ_k and Ψ_k are given by:

$$\Phi_k = \begin{pmatrix} I_d \\ \bar{A}_k \\ \bar{A}_{k+1} \cdot \bar{A}_k \\ \vdots \\ \bar{A}_{k+L-2} \cdot \bar{A}_{k+L-3} \cdot \ldots \bar{A}_k \end{pmatrix},$$

$$\Psi_k = \begin{pmatrix} 0 & 0 & \ldots & 0 \\ \bar{B}_k & 0 & \ldots & 0 \\ \bar{A}_{k+1} \cdot \bar{B}_k & \bar{B}_{k+1} & \ldots & 0 \\ \bar{A}_{k+2} \cdot \bar{A}_{k+1} \cdot \bar{B}_k & \bar{A}_{k+2} \cdot \bar{B}_{k+1} & \ldots & 0 \\ \vdots & \vdots & & \\ \bar{A}_{k+L-2} \cdot \ldots \bar{A}_{k+1} \cdot \bar{B}_k & \bar{A}_{k+L-2} \cdot \ldots \bar{A}_{k+2} \cdot \bar{B}_{k+1} & \ldots & \bar{B}_{k+L-1} \end{pmatrix},$$

Now equation (13) can be written in a more compact form using straightforward notation [Z_k and V_k denote the trajectories of z and v over the prediction horizon $[k, k+M]$]:

$$Z_k = \Phi_k \cdot z_k + \Psi_k \cdot V_k \tag{14}$$

This defines the linear system to which we adjoin the following cost function to define a model predictive control formulation:

$$\min_{V_k} \quad \left(Z_k^T \cdot Z_k + V_k^T \cdot R \cdot V_k \right) \tag{15}$$

The optimal sequence of actions is therefore obtained by the solution of (15) which is given by:

$$V_k^* = -(\Psi_k^T \cdot \Psi_k + 2 \cdot R)^{-1} \cdot \Psi_k^T \cdot \Phi_k \cdot W \cdot e_k$$

which by the very definition of model predictive control to the following time varying gain

$$K_k := -G \cdot (\Psi_k^T \cdot \Psi_k + 2 \cdot R)^{-1} \cdot \Psi_k^T \cdot \Phi_k \cdot W \tag{16}$$

where G is the matrix that selects the first control in the optimal sequence, namely $G = \begin{pmatrix} 1 & 0 & \ldots & 0 \end{pmatrix} \in \mathbb{R}^{1 \times L}$. Figure 5 shows the evolution of the components of K_k along the start-up time for a prediction horizon of $T = L \times \tau = 0.5$ sec and a sampling time of $\tau = 10$ ms (leading to a prediction horizon length of $L = 40$). The weighting matrix W is given by

$$W = \begin{pmatrix} I_d & 0 & 0 \\ 0 & 3 & 0 \\ 0 & 0 & 5 \end{pmatrix}$$

while the control weighting $R = 20 \times \mathbb{I}$ is considered. Note that the choice of the weighting matrix W imposes higher penalty on the speed Ω (gain = 5) since it is the main regulated variable. The second higher penalty is put on Q (gain = 3) because its stabilization enforces the stabilization of ξ [see (3)].

To summarize, during the start mode, the following time varying feedback law is applied to the plant

$$\gamma_k = \tilde{\gamma}_k + K_k \cdot e_k \tag{17}$$

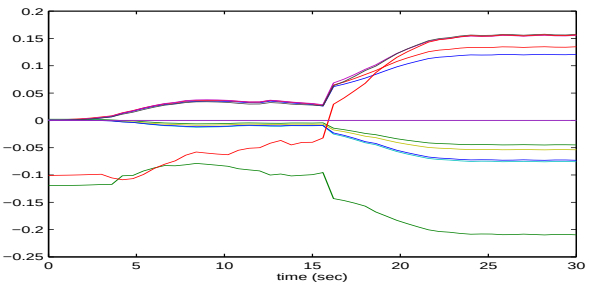

Fig. 5. Evolution of the components of K_k along the start-up time for a prediction horizon of $T = 0.5$ and a sampling period of $\tau = 10\ ms$ (prediction horizon length $L = 50$) used in the computation of the gain scheduling.

B. Closed-loop results

Figure 6 shows the closed-loop trajectory of the disturbed system (11) under the proposed feedback given by (17). This result shows that the feedback law enables the final desired state to be reached despite of the model discrepancy that have been introduced.

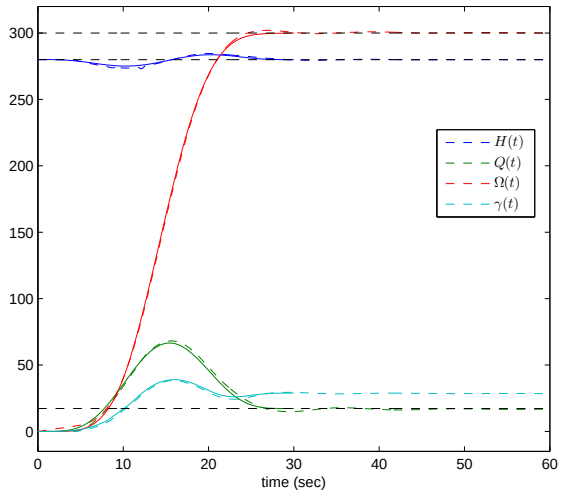

Fig. 6. desired trajectory computed trough process described in IV (solid line) and close loop results of the disturbed system (11) (dashed line)

In order to ensure robustness of such process, we checked the convergence of the system for the feedback law shown on Figure 5, and several values of perturbation. The table I sum-up the results of this analysis.

Uncertainties (%)	1	2.5	5
# tests conducted	3691	3602	3309
convergence of the system (%)	100	96.5	75.85
$\pm 0.2\%$ convergence mean time (s)	51.12	55.26	63.61

TABLE I

SUM-UP OF THE ROBUSTNESS ANALYSIS, THIS TABLE PROVIDES PERFORMANCES OF DEVELOPED FEEDBACK FOR SEVERAL THROWS OF THE UNCERTAIN SYSTEMS DESCRIBED AS IN (11) AND WITH DIFFERENT LEVELS OF UNCERTAINTIES.

VI. CONCLUSIONS

In this paper a method is proposed to achieve fast start-up of hydraulic turbines that are prone to "S" instability without misalignment of guide vanes. The method is based on a two step procedure. In the first step a fast steering trajectory that is compatible with the system constraints is generated based on the full nonlinear model of the turbine with its penstock. In the second step a gain-scheduling based tracking of the generated trajectory is proposed in which the computation of the gain profile is obtained through finite horizon predictive control that computes off-line the time varying components of the feedback gain. The efficiency of the proposed feedback is shown through simulations in which the nonlinear model is randomly detuned around its nominal behavior.

Undergoing work will address the reconstruction of the error vector through dedicated observers and the validation of the resulting closed-loop under noisy measurement. If the results show sensitive to measurement noise, the same approach will be specialized to the case of static output feedback control where only the main measured variables Ω, Q and H are involved in the correction term. To do this, a sparse identification of the feedback gain will be attempted in order to remove gains that affects unmeasured variables.

REFERENCES

[1] A. M. O. Haruni, A. Gargoom, M. E. Haque, and M. Negenvitsky. Dynamic operation and control of a hybrid wind diesel stand alone power systems. In Proceedings of the 25th IEEE Applied Power Electronics Conference and Exposition (APEC), pages 162169, 2010.

[2] M. Kalantar and G. Mousavi. Dynamic behavior of a stand-alone hybrid power generation system of wind turbine, solar array and battery storage, Applied Energy, 2010.

[3] ARTICLE 4383553, IEEE Std 125-2007 (Revision of IEEE Std 125-1988), IEEE Recommended Practice for Preparation of Equipment Specifications for Speed-Governing of Hydraulic Turbines Intended to Drive Electric Generators, 2007.

[4] Hui Sun, Ruofu Xiao, Weichao Liu, Fujun Wang, Analysis of S Characteristics and Pressure Pulsations in a Pump-Turbine With Misaligned Guide Vanes, College of Water Resources and Civil Engineering, China Agricultural University, 2013

[5] G. Orelind, L. Wozniak, J.Medanic, T. Whittmore, Optimal PID gain schedule for hydro-generators-design and application, IEEE Transaction on Energy conversion, 1989.

[6] Luz Alexandra Lucero Tenorio, Hydro Turbine and Governor Modeling. Electric - Hydraulic Interaction, Norwegian University of Science and Technology, 2010.

[7] Working Group on Prime Mover and Energy Supply, Hydraulic turbine and turbine control models for system dynamic studies, Transactions on Power Systems, Vol. 7, NO. 1, 1992

[8] P K Drfler R&D Department, Andritz Hydro Ltd., Zurich, Switzerland, Neo-Suterian pump-turbine characteristics and their benefits, 25th IAHR Symposium on Hydraulic Machinery and Systems, 2010.

[9] Jean-Bernard HOUDELINE, Jie LIU, Sylvain LAVIGNE, Yann LAURANT, Laetitia BALARAC, Start-up Improvement in Turbine mode for High Head PSP Machines. 26^{th} IAHR Symposium on Hydraulic Machinery and Systems, Beijing, China, 2012.

[10] K. Natarajan. Robust PID design for hydrauturbines. IEEE Transactions on Power Conversion, 20(3):661-667, 2005

[11] F. Yang, H. Lei, Y. Sun, W. Lin, and T. Shen. Control of hydraulic turbine generator using exact feedback linearization. In Proceedings of the 8th IEEE Conference on Control and Automation, 2010.